Plasmachemical Functionalization of Porous Polystyrene Beads

S. P. Godfrey, E. J. Kinmond, and J. P. S. Badyal*

Department of Chemistry, Science Laboratories, Durham University, Durham DH1 3LE, United Kingdom

I. R. Little

BP Amoco Chemicals, Sunbury-on-Thames, Middlesex TW16 7LL, United Kingdom

Received September 7, 2000. Revised Manuscript Received December 4, 2000

XPS, ATR-FTIR, ^{19}F MAS solid-state NMR, and imaging TOF−SIMS have been used to compare the depth and extent of chemical modification achieved during nonisothermal CF_4 plasma fluorination of nonporous, mesoporous, and microporous polystyrene spheres. It is shown that different depths of functionalization can be achieved by varying the polymer pore architecture. This methodology offers scope for preparing functionalized polymer supports and also protecting moisture-sensitive catalysts for handling in air.

1. Introduction

There is a growing interest in the use of polymers as supports for heterogeneous catalysis.[1−5] They offer several advantages compared to conventional inorganic oxide materials, including better control of pore architecture, processability, and inertness.[5] High surface area polystyrene supports and modified variants are particularly promising since it is possible to make these materials with a range of physical properties and incorporate a variety of functional groups onto the host polymer.[6] The latter is important because it is the chemical nature of the internal pore walls that governs the dispersion and anchoring of catalytic moieties. For instance, polystyrene resins have been shown to be effective at overcoming the detrimental interaction often observed between reactive metallocene polymerization catalysts and conventional silica supports.[1−4] In this context, fluorinated polystyrene derivatives potentially offer additional benefits related to enhanced thermal and chemical stability, thereby allowing highly sensitive catalysts to be supported for application under harsher reactor conditions.[5] A number of different approaches have been explored in the past aimed at making such supports; these have included copolymerization with a functionalized styrene[7] followed by tethering of the catalyst moiety[1−4] and direct fluorination of porous polystyrene spheres[5,8] via exposure to a fluorine/diluent gas mixture.[9] Cost is considered to be the major limiting factor in the former case, whereas safety, poor selectivity, and polymer degradation are drawbacks for the latter.[8,10]

A potentially safer, cheaper, cleaner, and quicker alternative is proposed comprising nonisothermal plasmachemical functionalization of high surface area polymer supports. Plasma treatment is know to be capable of reaching down to 1 μm for impermeable substrates,[11,12] whereas a greater penetration depth is possible for porous media.[13] This article describes a systematic investigation examining how polystyrene spheres with differing degrees of porosity are affected by CF_4 plasma fluorination. The depth and nature of chemical modification in each case has been evaluated by using a combination of elemental analysis, XPS, ATR-FTIR, ^{19}F MAS solid-state NMR, and imaging TOF−SIMS.

2. Experimental Section

Three different types of poly(styrene-*co*-divinylbenzene) beads were chosen to compare how depth of fluorination is affected by substrate porosity: nonporous beads (40-μm size, ≈2% divinylbenzene, Polyscience Inc.), mesoporous beads (30-μm particle size, pore size <50 nm, pore volume 65%, ≈36% divinylbenzene, Dyno Particles AS), and microporous beads (300−800-μm particle size, pore size <2 nm, pore volume 0.75 $cm^3\ g^{-1}$, ≈20% divinylbenzene, Aldrich). In the case of XPS and ATR-FTIR analysis, surface sensitivity was enhanced by grinding the large microporous beads to a size comparable to the other types of beads (≈10 μm) prior to plasma fluorination, whereas they were treated as a whole for bulk elemental

* To whom correspondence should be addressed.

(1) Roscoe, S. B.; Frechet, J. M. J.; Walker J. F.; Dias, A. J. *Science* **1998**, *280*, 270.
(2) Barrett A. G. M.; de Miguel, Y. R. *Chem. Commun.* **1998**, 2079.
(3) Chan, M. C. W.; Chew, K. C.; Dalby, C. I.; Gibson V. C.; Kohlmann, A.; Little I. R.; Reed, W. *Chem. Commun.* **1998**, 1673.
(4) Kitagawa, T.; Uozuni, T.; Soga K.; Takata, T. *Polymer* **1997**, *38*, 615.
(5) Wu, J. J.; Fu, L.; Chung, K. T. *Appl. Catal.* **1991**, *72*, 71.
(6) Lieto, J.; Milstein, D.; Albright, R. L.; Minkiewicz, J. V.; Gates, B. C. *Chemtech* **1983**, *13*, 46.
(7) Darling, G. D.; Frechet, J. M. J. *J. Org. Chem.* **1986**, *85*, 2270.
(8) Hewes, J. D.; Curren S.; Leone, E. A. *J. Appl. Polym. Sci.* **1994**, *53*, 291.
(9) Lagow, R. J.; Margrave, J. L. *Prog. Inorg. Chem.* **1979**, *26*, 161.
(10) Kharitonov, A. P.; Moskvin, Y. L. *J. Fluorine Chem.* **1998**, *91*, 87.
(11) Wildi, E. A.; Scilla, G. J.; DeLuca, A. *Mater. Res. Soc. Symp. Proc.* **1985**, *48*, 79.
(12) Loh I.-H.; Cohen, R. E.; Baddour, R. F. *J. Appl. Polym. Sci.* **1986**, *31*, 901.
(13) Yasuda, T.; Okuno, T.; Miyama, M.; Yasuda, H. *J. Polym. Sci., Polym. Chem.* **1994**, *32*, 1829.

10.1021/cm000722p CCC: $20.00
Published on Web 01/13/2001

analysis, ^{19}F MAS solid-state NMR, TOF−SIMS, and gas sorption studies.

Plasma fluorination experiments were carried out in a capacitively coupled 13.56-MHz Bio-Rad E2000 system, which had been fitted with a rotating powder holder controlled by a stepper motor. The reactor was continuously pumped by a 33 $dm^3\ h^{-1}$ Edwards E2M2 rotary pump via a liquid nitrogen cold trap to yield a base pressure of 1×10^{-2} mbar (leak rate better than 1×10^{-8} mol s^{-1}).[14] Prior to each experiment, the plasma chamber was scrubbed with detergent, rinsed with isopropyl alcohol, dried, and then cleaned further in situ using a 0.2-mbar air plasma at 40 W. Then, 0.5 g of polymer spheres was loaded into the reactor and evacuated down to base pressure. Next, CF_4 gas (Air Products, 99.7% purity) was introduced into the plasma chamber at a pressure of 0.4 mbar (equivalent to a flow rate of $8 \pm 1 \times 10^{-7}$ mol s^{-1}) via a fine needle valve. At this stage rotation of the reactor commenced and the gas discharge was ignited at 40 W. Upon completion of plasma treatment, the R. F. power supply was switched off, and CF_4 gas was allowed to continue to pass through the reactor for an additional 2 min, prior to evacuation back down to the original base pressure.

Bulk carbon, hydrogen, and nitrogen concentrations for each type of polymer bead were determined using an Exeter Analytical Inc. CE 440 elemental analyzer; this employed oxygen as the combustion gas and helium as the diluent. The level of fluorine incorporation achieved during plasma treatment was measured by carrying out sample combustion in an oxygen bomb, followed by dissolving the remains in aqueous solution and analyzing using a Dionex DX500 ion chromatogram.

The outer 2−5 nm of the polymer spheres were characterized by X-ray photoelectron spectroscopy (XPS)[15] using a VG ESCALAB MKII spectrometer fitted with an unmonochromatized Mg Kα X-ray source (1253.6 eV) and a hemispherical analyzer operating in the CAE mode (20-eV pass energy). The photoemitted core level electrons were collected at a takeoff angle of 30° from the substrate normal. Instrumentally determined sensitivity factors for unit stoichiometery were taken as C(1s):F(1s) = 1.00:0.23 (this assumes a homogeneous layer of uniform composition). For this technique, the polystyrene beads were embedded into indium foil (Aldrich, 99.99%) and then mounted onto the sample manipulator.

Attenuated total reflectance (ATR) FTIR spectroscopy was used to probe down to ≈4−5 μm below the surface.[16] Infrared absorption spectra were acquired using a Mattson Polaris spectrometer fitted with a Greasby Specac Golden Gate ATR accessory. The scan range was 600−4000 cm^{-1} at a resolution of 4 cm^{-1}; typically, 32 scans were averaged and the background was subtracted.

The overall chemical nature of the CF_4 plasma fluorinated polymer beads was determined by ^{19}F magic angle spinning (MAS) solid-state NMR spectroscopy. This was performed on a Varian Unity Plus 300-MHz spectrometer. Two hundred sixty transients were acquired using a 90° pulse, 5-s recycle delay, 200.0-kHz spectral width, and a magic angle spinning speed in excess of 16 kHz.

Cross-sectional microtoming required the polystyrene beads to be mounted in one of two ways: nonporous and microporous spheres were embedded into a thermoplastic adhesive (Tempfix, Agar scientific) at 383 K, while the smaller mesoporous spheres were fixed between a double layer of adhesive tape (3M, type 666). The samples were then sliced at 243 K using a cryogenic microtoming apparatus (Leica RM 2165).

Uncut and fractured beads were examined by optical microscopy and also coated with a thin layer of gold to enable characterization by a CamsScan Series 2 scanning electron microscope.

Table 1. BET Surface Area of the Polymer Beads

sample	untreated/$m^2\ g^{-1}$	fluorinated/$m^2\ g^{-1}$
nonporous[a]		
mesoporous	271.3 ± 2	268.2 ± 2
microporous[b]		

[a] Below nitrogen adsorption detection limit. [b] Microporous substrates do not fit the BET equation due to micropore filling.[43] However, the nitrogen gas absorption profile did not change.

Table 2. Bulk versus Surface Elemental Analysis

	bulk analysis		XPS
substrate	H:C	F:C	F:C
nonporous	1.0	0	0
nonporous CF_4 treated	1.0	0.002 ± 0.001	0.78 ± 0.03
mesoporous	1.1	0	0
mesoporous CF_4 treated	1.1	0.061 ± 0.006	0.84 ± 0.04
microporous	1.0	0	0
microporous CF_4 treated	1.0	0.014 ± 0.001	0.76 ± 0.05

TOF−SIMS analysis was carried out with a Physical Electronics 7200 instrument, which has been described previously.[17] A liquid metal ion gun was used for imaging (25 keV of Ga^+) with a submicron spot size (≈0.5 μm). The total dose was kept well under 10^{13} ions cm^{-2} (static conditions).

The porosity of the polystyrene beads before and after CF_4 plasma treatment was determined by nitrogen gas sorption measurements carried out at liquid nitrogen temperature using a PMI sorptometer. Only the mesoporous beads were found to obey the BET relationship[18] by showing a constant BET gradient over the range $0.04 < p/p_o < 0.25$.

3. Results

Nitrogen gas absorption characterization confirmed that no loss of porosity occurred during CF_4 plasma treatment of the microporous and mesoporous spheres (Table 1).

Bulk elemental analysis of the untreated polystyrene beads yielded hydrogen-to-carbon ratios approximately equal to the expected theoretical value of 1.0, based on the polymer structure (Table 2). The overall level of bulk fluorination obtained by CF_4 plasma treatment was found to correlate to the porosity of the polystyrene spheres as follows: nonporous < microporous < mesoporous.

Surface elemental composition calculated from the XPS peak areas gave similar F:C ratios for all three types of beads (no other elements were detected by this technique) (Table 2). Comparison with the bulk elemental analysis data suggests that in all cases the extent of fluorination is greater in the surface region relative to the bulk. The corresponding C(1s) XPS spectra of the untreated polystyrene spheres showed the presence of only $\underline{C}_xH_y$ groups at 285.0 eV, together with a weak $\pi-\pi^*$ shake-up satellite at 291.6 eV[19] (Figure 1). CF_4 plasma fluorination gave rise to a significant shift of the C(1s) envelope toward higher binding energies, indicating the formation of $\underline{C}-CF_n$ (286.6 eV), $\underline{C}F$ (287.6 eV), $\underline{C}F-CF_n$ (289.3 eV), $\underline{C}F_2$ (291.2 eV), and $\underline{C}F_3$ (293.3 eV) environments (additional Mg $K\alpha_{3,4}$ satellite features were displaced from their parent peaks by ≈9 eV toward

(14) Ehrlich, C. D.; Basford, J. A. *J. Vac. Sci. Technol., A* **1992**, *10*, 1.

(15) Briggs, D.; Seah, M. P. *Practical Surface Analysis, Volume 1-Auger and X-ray Photoelectron Spectroscopy*, 2nd ed.; John Wiley and Sons: Chichester, 1983.

(16) *Sampling Techniques for Infrared Analysis*; Graseby Specac Ltd.: Orpington, England, 1997; p 14.

(17) Boyd, R. D.; Kenwright, A. M.; Briggs, D.; Badyal, J. P. S. *Macromolecules* **1997**, *30*, 5429.

(18) Branauer, S.; Emmett, P. H.; Teller, E. *J. Am. Chem. Soc.* **1938**, *60*, 309.

(19) Clark, D. T.; Thomas, H. R. *J. Polym. Sci., Polym. Chem. Ed.* **1978**, *16*, 791.

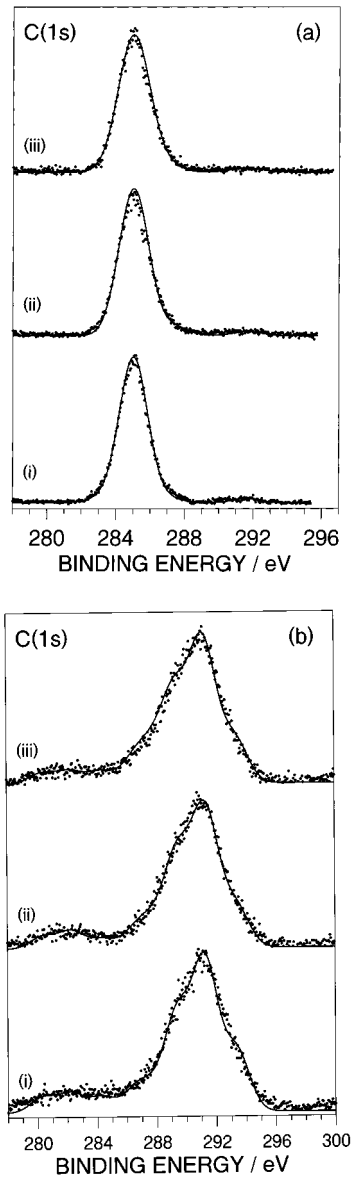

Figure 1. C(1s) XPS spectra of polystyrene beads: (a) untreated and (b) following CF_4 plasma treatment. Where the different types of bead are (i) nonporous, (ii) mesoporous, and (iii) microporous. (NB the solid lines represent the fitted data.)

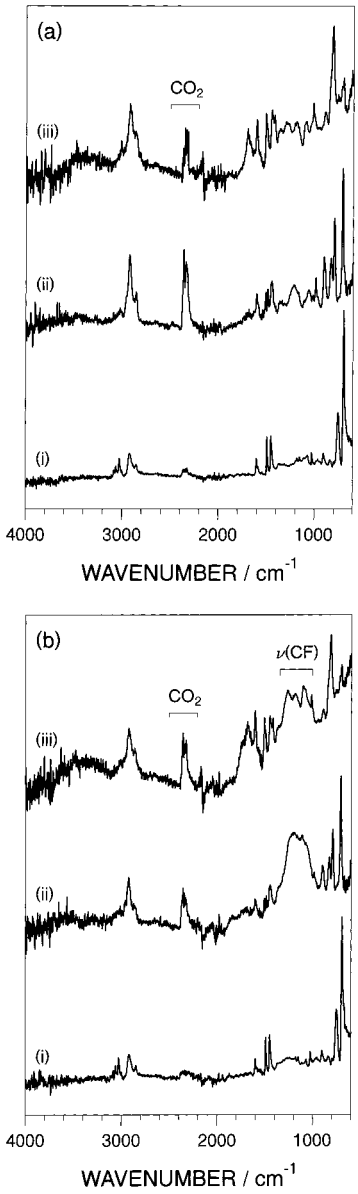

Figure 2. ATR−FTIR spectra of polystyrene beads: (a) untreated and (b) following CF_4 plasma treatment. Where the different types of bead are (i) nonporous, (ii) mesoporous, and (iii) microporous. (The CO_2 absorption band is attributed to background CO_2 gas contained within the pores.)

lower binding energy[20]). These surfaces were found to be stable over a period of 6 months.

Contrary to XPS, no change could be detected following plasma fluorination for the nonporous beads by ATR-FTIR (Figure 2), whereas the mesoporous and ground microporous polymer beads gave rise to a new absorption feature in the 1200−1400-cm^{-1} range associated with ($C-F_x$) functionalities[21] (Table 3). However, it is difficult to distinguish between the CF, CF_2, and CF_3 environments because of band overlap.[22] On this basis, it is clear that fluorination occurs at least down to the sampling depth of ATR-FTIR (4−5 μm)[16] for the mesoporous and microporous polystyrene spheres.

Table 3. Assignment of the IR Spectra[44]

vibrational mode	wavenumber/cm^{-1}
phenyl ring C−H stretching modes	3029, 3138
symmetric CH_2 stretching mode	2923
antisymmetric CH_2 stretching mode	2851
ring skeleton in-plane bend or stretch	1606, 1493, 1450
symmetric C−F stretching mode	1400−1200
ring in-plane C−C−H bending	1154, 1070, 1027
ring out-of-plane deformation	906, 842, 760, 700

The low overall level of fluorination previously seen by bulk elemental analysis and ATR-FTIR for the nonporous beads was confirmed by the absence of any signal during solid-state ^{19}F magic angle spinning NMR analysis, whereas both the mesoporous and microporous polymer spheres display three distinct regions: a broad feature between −30 and −90 ppm associated with CF_3

(20) Beamson, G.; Briggs, D. *High-Resolution XPS of Organic Polymers: The Scienta ESCA 300 Database*; John Wiley and Sons: Chichester, 1992.

(21) Painter, P. C.; Coleman, M. M.; Koenig, J. L. *The Theory of Vibrational Spectroscopy and its Application to Polymeric Materials*; John Wiley and Sons: New York, 1982.

(22) Lin-Vien, D.; Colthup, N. B.; Fateley, W. G.; Grasselli, J. G. *The Handbook of Infrared and Raman Characteristic Frequencies of Organic Materials*; Academic Press: London, 1991.

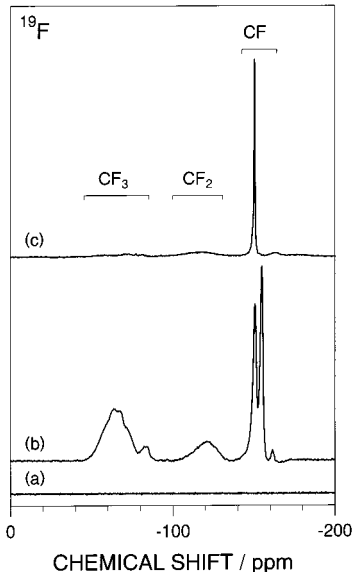

Figure 3. ^{19}F MAS NMR spectra of the fluorinated beads: (a) nonporous; (b) mesoporous; (c) microporous.

groups,[23−25] a band between −100 and −130 ppm due to $C\underline{F}_2$ groups,[23,26] and a resonance around −150 ppm attributed to aromatic $C\underline{F}$ groups,[27,28] Figure 3. The $C\underline{F}_3$ and $C\underline{F}_2$ signals appear to be more intense for the mesoporous beads than for the microporous beads.

Optical microscopy was used to verify that the larger microporous and nonporous beads could be fractured open by cryogenic microtoming. Scanning electron microscopy confirmed that this was also possible for the smaller mesoporous particles (Figure 4).

$^{19}F^-$ TOF−SIMS images of the untreated polystyrene beads taken after microtoming confirmed the absence of any fluorine within the bulk. Cross-sectioning of the plasma fluorinated nonporous polystyrene spheres showed fluorination at the surface only. Chemical modification was evident down to a depth of ≈5 μm for the microporous beads (Figure 5), while fluorination was discernible throughout the whole bulk of the mesoporous spheres (Figure 6).

4. Discussion

Chemistry at the plasma−solid interface comprises reaction of the substrate with ions, free radicals, excited species, electrons, and electromagnetic radiation contained in the plasma.[29] The high concentration of fluorine atoms present in a CF_4 plasma,[30−32] (together with a small number of CF, CF_2, and CF_3 radicals) can readily react with a polymer surface to yield CF, CF_2, and CF_3 functionalities.[33,34] Deposition is not a complication under these circumstances.[30,35] The observed absence of bulk fluorination for the nonporous polystyrene beads is consistent with previous studies using fluidized bed plasma reactors, which showed that only the surface is modified in the case of nonporous polyethylene and polystyrene beads.[12,36,37] However, plasma fluorination of the subsurface region readily occurs for the mesoporous and microporous polystyrene spheres. Plasma ignition throughout the bulk of such materials is unlikely because their pore dimensions (microporous <2 nm and mesoporous <50 nm) are much smaller compared to the characteristic plasma Debye length (2 μm < λ_D < 7 mm) of the electrical discharge.[29,38] Chemical reaction with the internal pore wall surfaces must therefore be occurring via diffusion of reactive species across the plasma−solid interface. Ion and

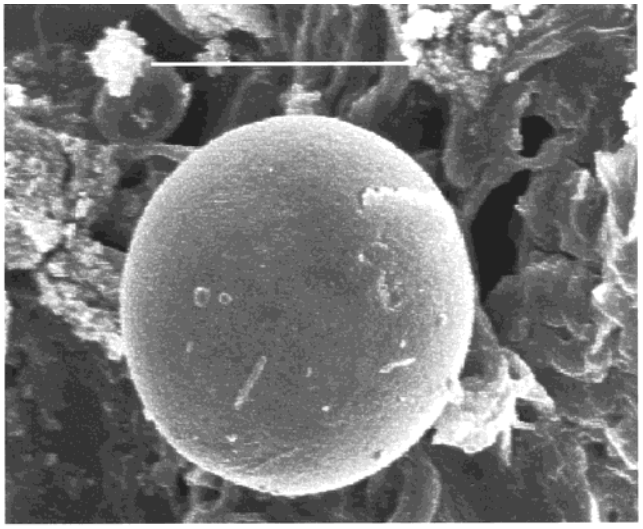

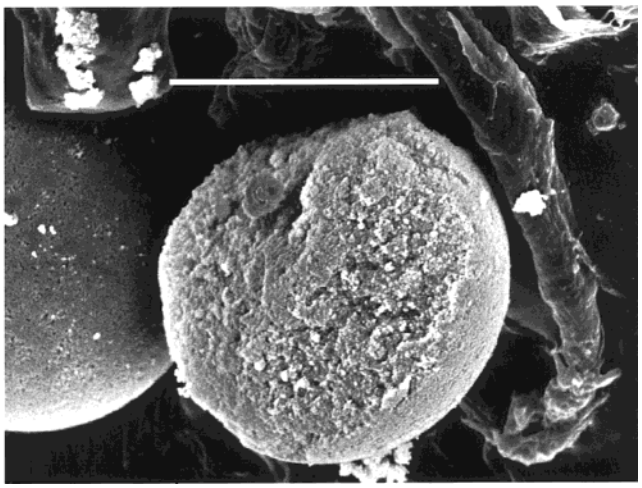

Figure 4. SEM images of 30-μm mesoporous polystyrene beads: (a) whole and (b) microtomed. (Scale bar = 20 μm.)

(23) Harris, R. K.; Jackson, P. *Chem. Rev.* **1991**, *91*, 1427.
(24) Tonelli, C.; Tortelli, V. *J. Fluorine Chem.* **1994**, *67*, 125.
(25) Tortelli, V.; Tonelli, C.; Corvaja, C. *J. Fluorine Chem.* **1993**, *60*, 165.
(26) English, A. D.; Garza, O. T. *Macromolecules* **1979**, *12*, 351.
(27) Toscano, P. J.; Waechter, J.; Schermerhorn, E. J.; Zhoue, P.; Frish, H. J. *J. Polym. Sci., Polym. Chem.* **1993**, *31*, 859.
(28) Carvalho de Mederios, M. A.; Cosnier, S.; Devonzier, A.; Moutet, J.-C. *Inorg. Chem.* **1996**, *35*, 2659.
(29) Grill, A. *Cold Plasmas in Materials Technology*; IEEE Press: New York, 1994.
(30) Truesdale, E. A.; Smolinsky, G. *J. Appl. Phys.* **1979**, *50*, 6594.
(31) McCaulley, J. A.; Goldberg, H. A. *J. Appl. Polym. Sci.* **1994**, *53*, 543.
(32) Edelson, D.; Flamm, D. L. *J. Appl. Phys.* **1984**, *56*, 1522.
(33) Strobel, M.; Corn, S.; Lyons, C. S.; Korba, G. A. *J. Polym. Sci. Polym. Chem.* **1985**, *23*, 1225.
(34) Occhiello, E.; Morra, M.; Garbassi, F.; Bargon, J. F. *Appl. Surf Sci.* **1989**, *36*, 285.
(35) Wang, J. Q.; Feng, D. M.; Wang, H. Z.; Rembold, M.; Thommen, F. *J. Appl. Polym. Sci.* **1993**, *50*, 585.
(36) Arand, M.; Cohen, R. E.; Baddour, R. F. *Polymer* **1981**, *22*, 361.
(37) Park, S. H.; Kim, S. D. *Polym. Bull.* **1998**, *41*, 479.
(38) Chapman, B. N. *Glow Discharge Processes*; John Wiley and Sons: New York, 1980.

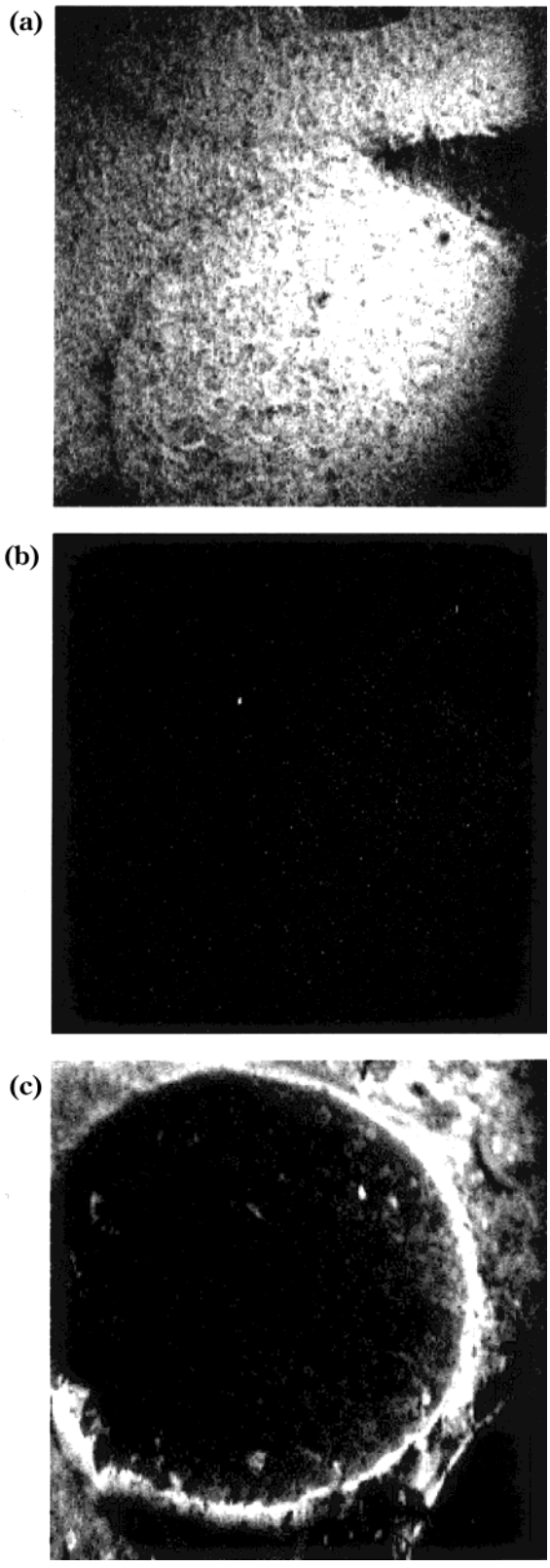

Figure 5. $^{19}F^-$ TOF imaging SIMS of microporous polystyrene beads: (a) total ion image of fractured untreated spheres; (b) F^- ion image corresponding to (a); (c) F^- ion image of fractured plasma-treated spheres (fluorination is observable down to a depth of 5 μm, which corresponds to the narrowest region of the white rim). (Scale = 500 μm.)

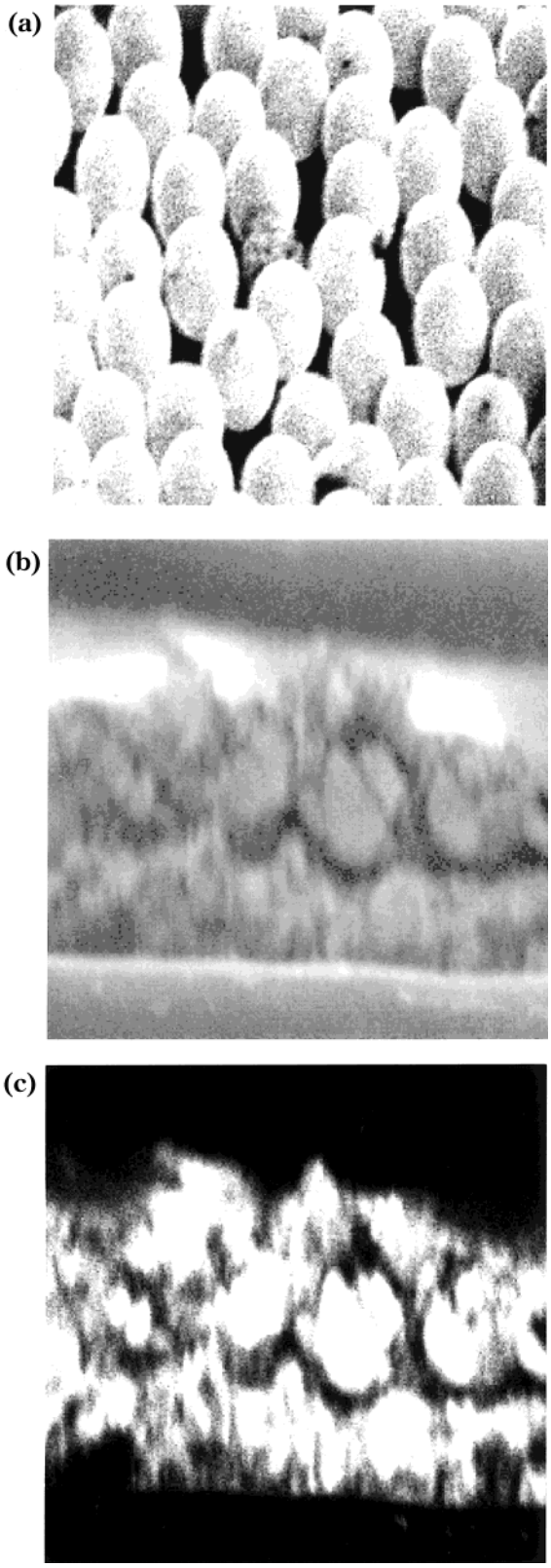

Figure 6. $^{19}F^-$ TOF imaging SIMS of mesoporous polystyrene beads: (a) F^- ion image of unfractured plasma-treated spheres; (b) total ion image of fractured plasma-treated spheres (the tape on either side of the particles is visible); (c) F^- ion image corresponding to (b) where fluorination can be observed throughout the particle cross sections located between the two pieces of tape. (Scale = 200 μm.)

electron penetration will be restricted to the near-surface region due to rapid loss of kinetic energy during collisions with the outer pore walls. This leaves atomic fluorine to diffuse into the subsurface via Knudsen flow since the pore diameters are smaller than the mean free

path of the excited plasma gas (≈100 μm).[39,40] Previous studies support this explanation since it has been shown that atomic fluorine can penetrate through multiple layers of fabric.[13] Therefore, the predominant mechanism for subsurface fluorination of the porous polymer spheres is via atomic fluorine attack.

The divinylbenzene linkages are effectively part of the polystyrene chain network (Structure 1); hence, the

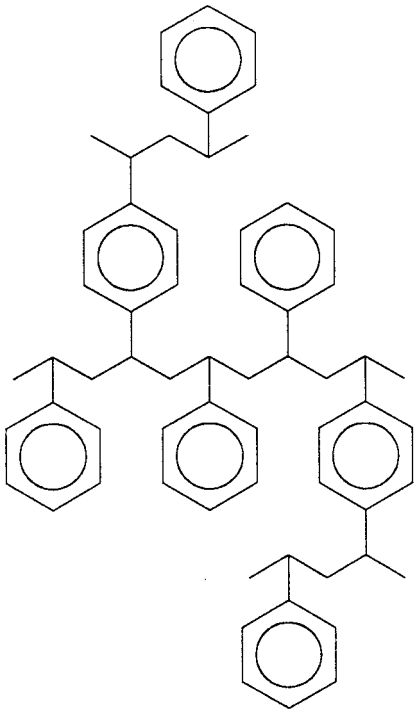

Structure 1: Divinylbenzene crosslinkages in the polystyrene beads

thermodynamically favored reaction pathways will be substitution of C−H bonds to form C−F linkages, together with fluorine addition across carbon−carbon double bonds located in the phenyl centers.[11,41,42]

A quantitative evaluation of the bulk and surface CF_x environments can be made by comparing the ^{19}F magic angle spinning NMR and XPS data (Table 4). The outermost 2-nm sampling depth of XPS consists primarily of CF_2 functionalities, whereas the bulk contains predominantly CF groups in the case of the microporous spheres and a mixture of CF, CF_2, and CF_3 groups for the mesoporous material. The greater level of fluorination at the surface can be explained in terms of a higher flux of reactive species in this region as well as the scope for additional reactions to proceed at the plasma−solid interface involving ions, electrons, and VUV photons. The greater depth and level of chemical modification measured for the mesoporous beads compared to its microporous counterpart can be attributed to the pore size of the former being ≈25 times wider as well as the plasma−solid interface being nearly 100 times greater in magnitude due to its smaller overall size.

Table 4. Comparison between ^{19}F MAS NMR and XPS C(1s) Spectra of CF_4 Plasma Fluorinated Mesoporous and Microporous Beads

		% fluorinated carbon		
substrate	technique	(CF + CF−CF_n)	CF_2	CF_3
mesoporous	^{19}F MAS NMR	67 ± 2	10 ± 3	23 ± 3
	XPS	37 ± 2	50 ± 3	13 ± 2
microporous	^{19}F MAS NMR	85 ± 2	12 ± 2	3 ± 1
	XPS	38 ± 3	47 ± 5	15 ± 3

The observed limited depth of plasma fluorination associated with the microporous polystyrene beads could potentially find application for the preparation of polymer-supported moisture-sensitive catalysts, where the outer fluorinated region of the polymer bead is formed after catalyst impregnation. This would prevent any subsequent permeation of moisture toward the "soft center", that is, provide a means for the storage and transportation in air of moisture-sensitive supported catalysts. Each polymer bead "capsule" could then be opened up by solvent swelling under reactor conditions.

5. Conclusions

The size and porosity of polystyrene spheres govern their susceptibility toward plasma fluorination. Microporous beads can be functionalized to a depth of ≈5 μm, whereas mesoporous polystyrene particles are chemically modified throughout the bulk.

Acknowledgment. S.P.G. is grateful to EPSRC and BP Amoco Chemicals for a Ph.D. studentship. We would like to thank D. C. Apperley and I. Fletcher for carrying out the solid-state NMR and TOF−SIMS experiments, respectively.

CM000722P

(39) Thomas, J. M.; Thomas, W. J. *Introduction to the Principles of Heterogeneous Catalysis*; Academic Press: London, 1967.
(40) Atkins, P. W. *Physical Chemistry*, 4th ed.; Oxford University Press: Oxford, 1990; Chapter 24.
(41) Hopkins, J.; Badyal, J. P. S. *J. Phys. Chem.* **1995**, *99*, 4261.
(42) Strobel, M.; Thomas, P. A.; Lyons, C. S. *J. Phys. Chem.* **1987**, *25*, 3343.
(43) Gregg, S. J.; Sing, K. S. W. *Adsorption, Surface Area and Porosity*; Academic Press: London, 1967; Chapter 4.
(44) Bower, D. I.; Maddans, W. F. *The Vibrational Spectroscopy of Polymers*; Cambridge University Press: Cambridge, 1989.